

## TiO<sub>2</sub>-modified zeolite-carbon nanotubes composite electrode for photoelectrodegradation of pentachlorophenol from water under uv irradiation

Jakab, Agnes; Pode, Rodica; Pop, Aniela; Schoonman, Joop; Orha, Corina; Manea, Florica

**DOI**

[10.2495/WS170121](https://doi.org/10.2495/WS170121)

**Publication date**

2017

**Document Version**

Final published version

**Published in**

WIT Transactions on Ecology and the Environment

**Citation (APA)**

Jakab, A., Pode, R., Pop, A., Schoonman, J., Orha, C., & Manea, F. (2017). TiO<sub>2</sub>-modified zeolite-carbon nanotubes composite electrode for photoelectrodegradation of pentachlorophenol from water under uv irradiation. *WIT Transactions on Ecology and the Environment*, 216, 133-142. <https://doi.org/10.2495/WS170121>

**Important note**

To cite this publication, please use the final published version (if applicable). Please check the document version above.

**Copyright**

Other than for strictly personal use, it is not permitted to download, forward or distribute the text or part of it, without the consent of the author(s) and/or copyright holder(s), unless the work is under an open content license such as Creative Commons.

**Takedown policy**

Please contact us and provide details if you believe this document breaches copyrights. We will remove access to the work immediately and investigate your claim.

# TiO<sub>2</sub>-MODIFIED ZEOLITE-CARBON NANOTUBES COMPOSITE ELECTRODE FOR PHOTOELECTRODEGRADATION OF PENTACHLOROPHENOL FROM WATER UNDER UV IRRADIATION

AGNES JAKAB<sup>1</sup>, RODICA PODE<sup>1</sup>, ANIELA POP<sup>1</sup>, JOOP SCHOONMAN<sup>2</sup>, CORINA ORHA<sup>3</sup>, FLORICA MANEA<sup>1</sup>

<sup>1</sup>Politehnica University of Timisoara, Romania,

<sup>2</sup>Department of Chemical Engineering, Delft University of Technology, The Netherlands

<sup>3</sup>National Institute for Research and Development in Electrochemistry and Condensed Matter, Romania

## ABSTRACT

Three types of composite electrode materials, i.e. carbon nanotubes-epoxy (CNT), zeolite-carbon nanotubes-epoxy (ZCNT) and TiO<sub>2</sub>-modified zeolite-carbon nanotubes-epoxy (TiZCNT), were synthesized, morphologically and electrically characterized, and tested in the photoelectrodegradation of pentachlorophenol (PCP) from water. The electrode composite materials were synthesized by the two-roll mill method, and a higher porosity of zeolite-modified electrode, caused by the zeolite incorporation, was noticed by means of scanning electron microscopy. Electroactive surface area, determined by classical methods using cyclic voltammetry (CV), and electric conductivity, determined by the four-point method, were negatively affected by the presence of zeolite. The photoelectrochemical behaviour of the electrodes, under ultraviolet (UV) irradiation, towards the pentachlorophenol oxidation was studied, and the photoelectrocatalytic activity of each electrode was determined. The PCP oxidation occurred in two steps at +0.65 V and +0.94 V vs. saturated calomel electrode SCE under UV irradiation. The oxidation peak recorded at +0.65 V vs. SCE appeared only under UV irradiation and it is considered that the photoelectrooxidation peak corresponded to PCP photoelectrooxidation. Also, the enhancement of PCP electrooxidation at +0.94 V vs. SCE was noticed under UV irradiation, which confirmed the photoelectrocatalytic activity. The performance of the PCP degradation process, expressed as degradation efficiency and electrochemical efficiency, recommended the operation of photoelectrocatalysis at a bias voltage application of +0.8 V/SCE, while the mineralization degree recommended a bias voltage value of +1.5 V/SCE.

*Keywords: wastewater treatment, pentachlorophenol, TiO<sub>2</sub>-modified zeolite-carbon nanotubes-epoxy composite electrode, photoelectrodegradation.*

## 1 INTRODUCTION

Untreated wastewater can exhibit a catastrophic impact on an ecosystem and human health via the water cycle. Continuous research to develop and implement new and emerging technologies is supported by the measures and actions proposed through the Water Framework Directive. The class of priority organic pollutants in wastewaters is very common in industrialized countries; these pollutants constitute a serious environmental problem because of their toxicity [1]–[3] and carcinogenic effects on human health [4]–[6]. The biological degradation process is a common step in wastewater treatment technology to degrade the organic loading from water, but, because of the resistance to biodegradation of priority pollutants, other water treatment processes should be applied.

In the last decade, special attention has been given to advanced oxidation processes (AOPs) for the degradation and mineralization of organic pollutants that resist biological treatment. These processes refer to oxidative water treatments, which involve the generation of very reactive oxygen species, able to rapidly attack and destroy the pollutants [7]–[12]. A



main innovation is the combination of different advanced oxidation processes and appropriate post-treatment technologies, called hybrid oxidation processes [13].

Both the electrochemical and the photocatalytic processes are AOPs, but their combination has received growing attention. Thus, for the degradation of pollutants from water, the combination of electrochemical and photocatalysis processes, such as photoelectrocatalysis [14] and electrochemically-assisted photocatalysis [15] processes, have been reported. The main difference between these variants is denoted by which of these represents the core process. For any presented variants, the operational parameters of the electrochemical process are most responsible for the efficiency of the overall process. Also, the type of photocatalyst makes a major contribution to the process performance.

TiO<sub>2</sub> and other n-type semiconductors are applied as photocatalysts for the effective degradation and mineralization of target compounds [16]. It is well-known that the photocatalysis process is based on the generation of electron-hole pairs, while electrochemical oxidation produces the hydroxyl radical directly on the electrode surface or indirectly via oxygen evolution. For the photoelectrochemical process, the photogenerated electrons are produced by applying bias voltage and, thus, the photodegradation is enhanced through more effective separation of photogenerated charges by increasing the lifetime of electron-hole pairs [16].

Due to their chemical stability and good electrical conductivity, carbon nanotubes (CNTs) are used as electrodes and/or as a support for the dispersion of functional materials [17] in order to obtain a large surface area, better catalyst dispersion and high electroactivity [18]. Also, natural mineral materials, such as the eco-friendly and low-cost zeolites, have excellent properties that can be exploited for electrochemical applications. Due to these properties, e.g. ion-exchange capacity, molecular selectivity, catalyst-assisted reactivity, microporous structure and conductivity, they are frequently used in composite electrodes [19], [20].

In this study, three types of composite electrode materials, *i.e.*, carbon nanotubes-epoxy (CNT), zeolite-carbon nanotubes-epoxy (ZCNT) and TiO<sub>2</sub>-modified zeolite-carbon nanotubes-epoxy (TiZCNT), were synthesized, morphologically and electrically characterized, and tested in the photoelectrodegradation of pentachlorophenol (PCP) from water in order to develop new technology for advanced water treatment.

## 2 MATERIALS AND METHODS

### 2.1 Materials

Multiwalled carbon nanotubes (CNTs), produced by a catalytic carbon vapor deposition method, were obtained from NanocylTM, Belgium. Carbon nanofibers (CNFs) (Pyrograf III-PR24 AGLD) were purchased from Applied Science Inc., Cedarville, Ohio, USA. The matrix system used was the epoxy resin, Araldite®LY5052, and its corresponding hardener, Aradur®5052, manufactured by Huntsman Advanced Materials, Switzerland. N,N-dimethylformamide (DMF) and tetrahydrofuran (THF) were used as solvents and were purchased from Sigma-Aldrich BV, Germany. Romanian zeolitic mineral from Mirșid, used as support for TiO<sub>2</sub>, was supplied by CEMACON Company, Romania. The precursor used for the synthesis of TiO<sub>2</sub> was titanium isopropoxide (TTIP, 98%) (Sigma-Aldrich, Germany).

### 2.2 Preparation of (TiO<sub>2</sub>-zeolite) carbon nanotubes-based epoxy composite electrodes

The methods used for the synthesis of the composite materials were the sol-gel (SG) and microwave-assisted hydrothermal route. The natural zeolite from the Mirșid area of Romania,



which was used, has the composition: 62.20% SiO<sub>2</sub>; 11.65% Al<sub>2</sub>O<sub>3</sub>; 1.30% Fe<sub>2</sub>O<sub>3</sub>; 3.74% CaO; 0.67% MgO; 3.30% K<sub>2</sub>O; 0.72% Na<sub>2</sub>O; and 0.28% TiO<sub>2</sub> (%wt.). In the first step, the dispersion of CNT/CNF in N,N-dimethylformamide (DMF) and tetrahydrofuran (THF), 99.8% was achieved by ultrasonication, using a Cole-Parmer® 750-Watt Ultrasonic Processor for about 10 min. After this sonication process, the obtained solution was mixed with TiO<sub>2</sub>-modified zeolite and sonicated again with epoxy resin to obtain a homogeneous mixture. The mixture was left overnight in a vacuum oven at 60°C in order to evaporate the solvent and remove the air bubbles. In the next processing step, the TiO<sub>2</sub>-modified zeolite-CNT-epoxy was subjected to a two-roll mill (TRM) process to achieve high levels of dispersion and distribution. During processing, the temperature was kept constant at 70°C, the mixing speed was maintained at 10 and 20 rpm for about 40 min and, subsequently, the curing agent (weight ratio of epoxy resin to curing agent was 100:38) was added to the mixture; mixing was then continued for an additional 20 min to ensure uniform dispersion within the sample. Finally, the resulting paste was poured into cylindrical PVC tubes, and electrical contact was assured using copper wire. These electrodes were cured in a vacuum oven at 80°C for 24h hours and subsequently left to cool down to room temperature. The electrode surfaces were polished before each experiment with a soft abrasive paper and rinsed with distilled water.

### 2.3 Electrode characterization and testing in PCP photoelectrodegradation

Morphological characterization of the composites was carried out using scanning electron microscopy (SEM XL20, Philips) with an acceleration voltage of 15 kV. The electrical conductivity of the carbon nanofiber-epoxy composite electrode was determined by a four-point probe (FPP) method based on DC conductivity measurements.

The electrochemical and photoelectrochemical experimental set-up consisted of a three-electrode quartz cell, an ultraviolet light source and an autolab potentiostat/galvanostat PGSTAT 302 (EcoChemie, The Netherlands) controlled with GPES 4.9 software. The potentiostat was connected with a Pt counter electrode, a reference electrode (saturated calomel electrode) and the carbon based composite working electrode.

Cyclic voltammetry (CV) technique was used to characterize the electrochemical and photoelectrochemical behaviours of the composite electrodes in the presence of PCP and 0.1 M Na<sub>2</sub>SO<sub>4</sub> supporting electrolyte. The photoelectrodegradation experiments were conducted under potentiostatic regime using the chronoamperometry (CA) technique

The PCP concentration before and after the degradation process was determined by a UV-spectrophotometric method, recorded at the wavelength of 218 nm, using a Varian Cary 100 UV-VIS Spectrophotometer.

The PCP degradation process efficiency,  $\eta$ , was determined based on eqn. 1:

$$\eta = \left[ \frac{(PCP_0 - PCP)}{PCP_0} \right] \times 100 (\%), \quad (1)$$

where  $PCP_0 - PCP$  is the change in the PCP concentration during degradation experiments.

In addition to the PCP removal process efficiency, the electrochemical efficiency for PCP oxidation,  $E_{\text{amper}}$ , was obtained based on eqn. 2 [21]:

$$E_{\text{amper}} = \left[ \frac{(PCP_0 - PCP)}{C \cdot S} \right] \cdot V \text{ (g / C} \cdot \text{cm}^2\text{)}, \quad (2)$$

where  $PCP_0 - PCP$  is the change in the PCP concentration during degradation experiments for a charge consumption of  $C$ , corresponding to a certain time;  $V$  is the sample volume (50 ml), and  $S$  is the area of the electrode (cm<sup>2</sup>).



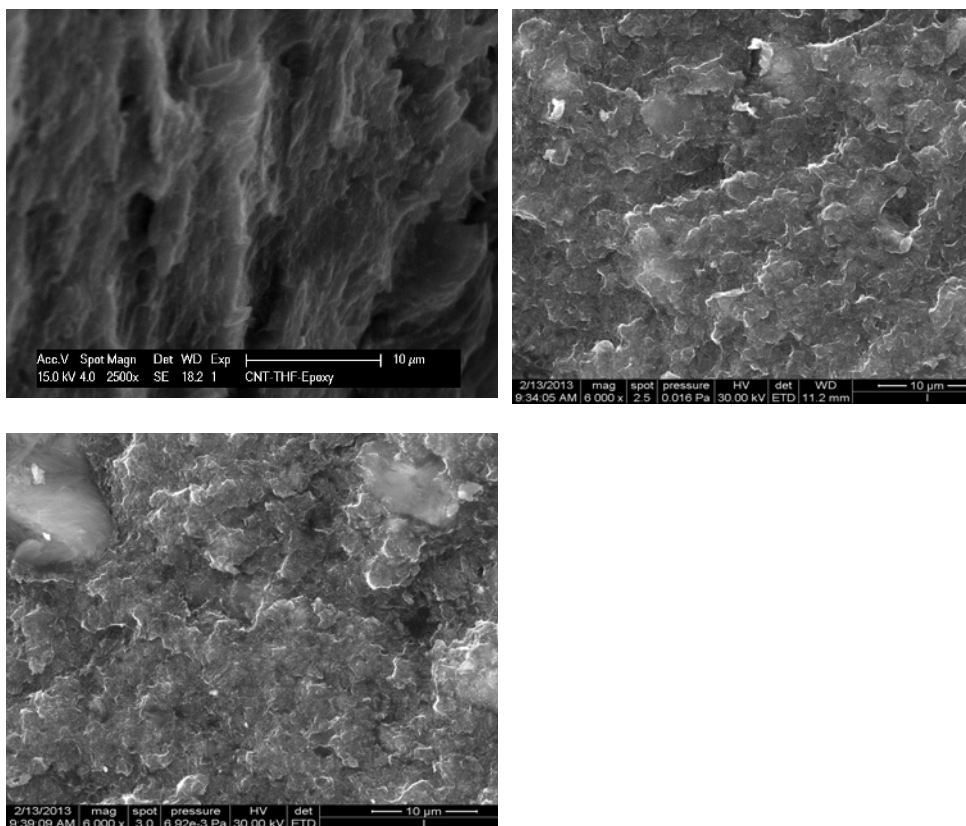


Figure 1: SEM image of the composite electrode materials: a) CNT, b) ZCNT, c) TiZCNT.

Table 1: Electrical conductivity of the composite electrode material.

Electrode material	Electrical conductivity, $S \cdot cm^{-1}$
CNT	0.596
ZCNT	0.237
TiZCNT	0.365

### 3 RESULTS AND DISCUSSION

Figure 1 shows comparative scanning electron microscopy (SEM) images of carbon nanotubes-based composite electrodes. A relatively good distribution of carbon nanotubes and zeolite within epoxy resin is noticed. The zeolite intercalation within the electrode composition gave a more porous morphology of the surface.

The electrical conductivity determined for each composite material is gathered in Table 1. The insulating zeolite material decreased the electrical conductivity of the composite material, but all values showed the materials' suitability to be applied in the electrochemical experiments. In comparison with the zeolite,  $TiO_2$  slightly enhanced the electrical conductivity of the material.

An important peculiarity of the electrode materials is the electroactive surface area that influences the electrochemical activity. The classical method, consisting of electroreduction–electrooxidation of the ferri/ferrocyanide system, is used to determine the electroactive surface area, based on the Randles–Sevcik equation, eqn. 3 [22]:

$$I_p = 2.69 \times 10^5 AD^{1/2} n^{3/2} \nu^{1/2} C, \quad (3)$$

where A represents the area of the electrode ( $\text{cm}^2$ ), n is the number of electrons participating in the reaction and is equal to 1, D is the apparent diffusion coefficient of the molecule in solution ( $\text{cm}^2\text{s}^{-1}$ ), C is the concentration of the probe molecule in the solution and is 4mM, and  $\nu$  is the scan rate ( $\text{V s}^{-1}$ ).

The values of the electroactive surface area are shown in Table 2, where the higher electroactive surface areas versus the geometrical areas for all composite electrode materials can be seen. Also, the presence of zeolite significantly decreased the electroactive surface area due to its insulating characteristic.

In order to select the most suitable electrode material for testing the photoelectrocatalytic performance for PCP degradation and mineralization, the cyclic voltammetry technique was tested under UV irradiation. The cyclic voltammograms, recorded at the TiZCNT electrode in the presence of various PCP concentrations ranging from 0 to 60  $\mu\text{M}$ , are presented in *Figure 2a*. In comparison with the results recorded under the same operational conditions but without UV irradiation (the results are not shown here), it must be underlined that the appearance of a new oxidation peak, recorded at lower potential value (+0.69 versus +0.90 V/SCE), is very promising for photoelectrodegradation applications. The oxidation peak for PCP oxidation appeared at +0.90 V without UV irradiation; this denotes that the electrocatalytic activity of the electrode material in respect of PCP oxidation, is also improved by UV irradiation. Using this methodology, the electrocatalytic activity under UV irradiation was determined and the results for all electrodes are presented in Table 3. Based on these results, TiZCNT is selected for further testing applications.

### 3.1 Testing TiZCNT in photoelectrodegradation of PCP from water

To demonstrate the potential practical application of TiZCNT, its ability to degrade PCP was investigated. The photoelectrodegradation experiment was performed under potentiostatic operational conditions, assured by using chronoamperometry (CA). Figures 3a-b show the photoelectrocatalytic degradation performance of PCP, expressed as degradation efficiency and electrochemical efficiency. Unlike degradation efficiency, electrochemical efficiency contains the energy consumption component, besides the technical aspect. The bias voltage applied in the photoelectrochemical degradation experiments was selected based on the above-presented CV results to assure the direct oxidation of PCP on the electrode surface (+0.8V/SCE) and in the range of  $\text{O}_2$  evolution (+1 and +1.5 V/SCE). The value of bias potential applied on the photocatalyst is the key to the operational parameters, bearing in mind both the electrochemical and photocatalytic processes, which compose the overall

Table 2: The electroactive surface areas ( $A_{\text{electro}}$ ) of the carbon nanotubes-based composite electrodes.

Type of electrode	$A_{\text{electroactive}} [\text{cm}^2]$	$A_{\text{geometrical}} [\text{cm}^2]$
CNT	0.898	0.196
ZCNT	0.308	0.196
TiZCNT	0.800	0.196



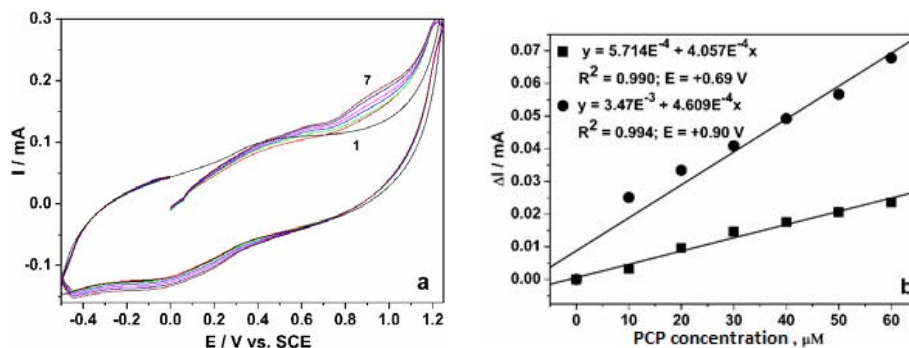


Figure 2: (a) Cyclic voltammety recorded at TiZCNT electrode under UV irradiation in 0.1 MNa<sub>2</sub>SO<sub>4</sub> and various PCP concentrations: 1-0  $\mu M$ ; 2-10  $\mu M$ ; 3-20  $\mu M$ ; 4-30  $\mu M$ ; 5-40  $\mu M$ ; 6-50  $\mu M$ ; 7-60  $\mu M$ ; potential range: -0.5 V  $\rightarrow$  +1.25 V vs. SCE; scan rate: 0.05 V $\cdot$ s<sup>-1</sup>; (b) Linear dependence of anodic peak current versus PCP concentrations ( $E = +0.69 V$  și  $E = +0.90 V$  vs. SCE).

Table 3: Photoelectrocatalytic performance of the electrode materials for PCP oxidation using CV.

Electrode material	Potential value V/SCE	Electrocatalytical activity under UV irradiation ( $\mu A/\mu M$ )
CNT	+0.94	0.625
	+0.67	0.332
ZCNT	+0.90	0.814
	+0.69	0.409
TiZCNT	+0.90	2.060
	+0.69	0.538

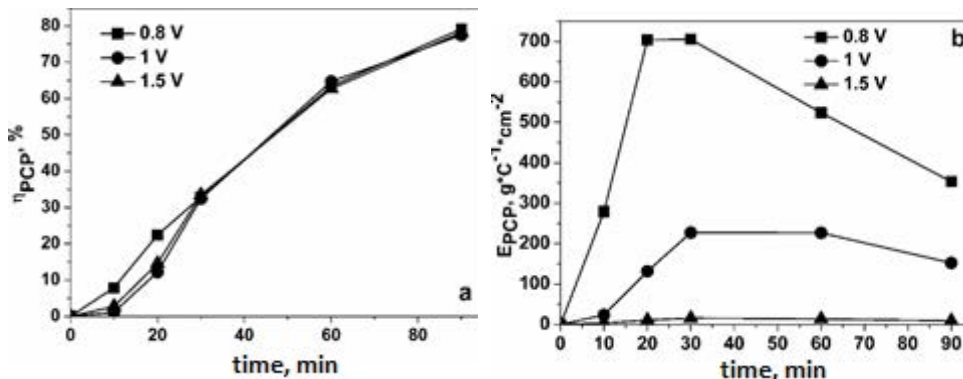


Figure 3: PCP degradation performance on TiZCNT electrode by photoelectrodegradation under UV irradiation and bias voltage of +0.8; +1; and +1.5 V/SCE, expressed as: a) Degradation efficiency; and b) Electrochemical efficiency.

photoelectrochemical process. Depending on the bias potential value, a hampering effect of each to the other process should have appeared or a sum of both processes, or their synergic effect. The main aim of the bias voltage application is to block the possible recombination of electron and hole, which represents the core of the photocatalysis process. The photoelectrodegradation performances, determined under all bias voltage values and expressed as a PCP degradation grade, showed similar results. However, a significant difference is noticed for electrochemical performance, with the best results being obtained for a bias voltage value of 0.8 V/SCE. Higher voltage applied more abundant O<sub>2</sub> evolution as secondary process that means lower current efficiency and higher energy-consuming. The evolution of the UV-VIS spectrum profile for PCP before and after photoelectrodegradation application, for bias voltage value of 0.8 V/SCE, is given in Fig. 4; notable are the major changes in the shape, which revealed the occurrence of the degradation process.

For a better assessment of the photoelectrodegradation, the kinetics studies were performed based on monitoring the UV-VIS spectrum evolution and also the total organic carbon (TOC) parameter that measured the mineralization evolution. The pseudo-first-order kinetic model fitted the best PCP degradation and mineralization process and is described by the simplified Langmuir-Hinshelwood equation:

$$\ln(C_0 / C_t) = kKt = k_{app}t, \quad (4)$$

where  $k_{app}$  is apparent rate constant, min<sup>-1</sup>.

The apparent rate constants and regression coefficients of PCP photoelectrocatalysis, in terms of degradation and mineralization, are shown in Table 4. The correlation coefficients higher than 0.9 for all applied systems revealed that the equation is suitable for kinetics

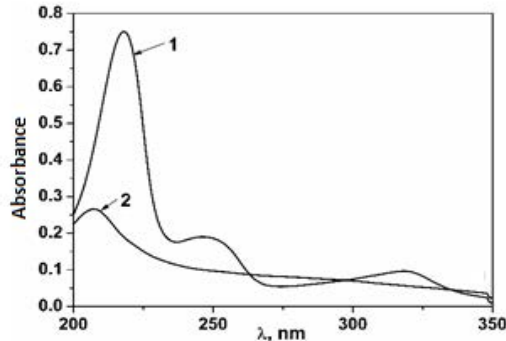


Figure 4: UV-VIS spectrum profile of PCP: 1-initial and 2-after 90 minutes of photoelectrodegradation.

Table 4: Kinetics parameters and correlation coefficients corresponding to PCP degradation at bias voltage value of +0.8; +1.0; +1.5 V vs. SCE; photoelectrodegradation time of 90 minutes.

Bias voltage value, V/SCE	Apparent rate constant, min <sup>-1</sup>		R <sup>2</sup>	
	$k_{app}$ degradation	$k_{app}$ mineralization	Degradation	Mineralization
+0.8	0.018	0.0062	0.996	0.907
+1.0	0.018	0.0093	0.990	0.923
+1.5	0.018	0.0112	0.993	0.924



aspects description. Rate constants were calculated to be  $18.00 \cdot 10^{-3} \text{ min}^{-1}$  for degradation and  $6.2 \cdot 10^{-3}$ ,  $9.3 \cdot 10^{-3}$  and  $11.2 \cdot 10^{-3} \text{ min}^{-1}$  for mineralization at bias voltage value of +0.8; +1.0 and +1.25 V/SCE, respectively. These results showed that, for higher bias voltage application, the mineralization degree is enhanced.

The selection of the bias voltage value is based on the concrete practical application and the integration of the process into the wastewater treatment flow. If this process constitutes the finishing step as advanced oxidation process that should ensure the pollutants' mineralization, a higher bias voltage is required, even if this means that the energy consumption is higher. If this process is integrated into wastewater treatment flow prior to the biological step, no mineralization is expected, but a conversion to more biodegradable compounds and a lower bias voltage is selected.

#### 4 CONCLUSIONS

Carbon nanotubes-epoxy (CNT), zeolite-carbon nanotubes-epoxy (ZCNT) and  $\text{TiO}_2$ -modified zeolite-carbon nanotubes-epoxy (TiZCNT) were synthesized successfully by the two-roll mill method. Electroactive surface area, determined by classical methods using cyclic voltammetry (CV), and electric conductivity, determined by the four-points method, were negatively affected by the presence of zeolite. However, electroactive surface areas higher than the geometrical areas were obtained for all synthesized electrode materials. The photoelectrochemical behaviour of the electrodes, under UV irradiation, towards the pentachlorophenol oxidation showed that the PCP oxidation occurred in two steps at about +0.65 V and +0.94 V vs. SCE. The oxidation peak recorded at +0.65 V vs. SCE appeared only under UV irradiation, is considered to be the photoelectrooxidation peak that corresponded to PCP photoelectrooxidation. Also, the enhancement of PCP electrooxidation at +0.94 V vs. SCE was noticed under UV irradiation, which confirmed the photoelectrocatalytic activity. The performance of the PCP degradation process, expressed as degradation efficiency and electrochemical efficiency, recommended the operation of photoelectrocatalysis at a bias voltage application of +0.8 V/SCE, while the mineralization degree recommended a bias voltage value of +1.5 V/SCE. The selection of the operational conditions is based on where integration of the photoelectrocatalysis takes place within the wastewater treatment technology flow: prior or after the biological step or as a single step. Although further study is needed to make TiZCNT-based photoelectrocatalysis proficient for practical application, this study was essential as the reference for process design at pilot scale and, further, at industrial scale.

#### ACKNOWLEDGEMENT

This work was supported by the Romanian National Research Programs, PN-III-P2-2.1-PED-2016, 69PED/2017 and PN-II-TE-123/2015.

#### REFERENCES

- [1] Igbinsa, E.O. et al., Toxicological profile of chlorophenols and their derivatives in the environment: the public health perspective. *Scientific World Journal*, **22**(2), pp. 1-11, 2013.
- [2] Agbo, S.O., Kuester, E., Georgi, A., Akkanen, J., Leppanen, M.T. & Kukkonen J.V.K., Photostability and toxicity of pentachlorophenol and phenanthrene. *Journal of Hazardous Materials*, **189**, pp. 235-240, 2011.
- [3] Kim, J.K., Choi, K., Cho, I.H., Son, H.S. & Zoh, K.D., Application of a microbial toxicity assay for monitoring treatment effectiveness of pentachlorophenol in water



- using UV photolysis and TiO<sub>2</sub> photocatalysis. *Journal of Hazardous Materials*, **148**, pp. 281-286, 2007.
- [4] McLellan, I. et al., The environmental behaviour of polychlorinated phenols and its relevance to cork forest ecosystems: a review. *Journal of Environmental Monitoring*, **9**(10), pp.1055-1065, 2007.
- [5] Wang, J., (ed.), *Analytical Electrochemistry*, Wiley-VCH: New York, 2000.
- [6] Vanloon, G.W. & Duffy, J.S., (eds), *Environmental Chemistry. A global perspective*, Oxford University Press: Oxford, p. 492, 2000.
- [7] Kommineni, S., Zoeckler, J., Stocking, A., Liang, S., Flores, A. & Kavanaugh, M., Advanced oxidation processes. *National Water Research Institute*, pp. 111- 208, 2008.
- [8] Comminellis, C.H., Kapalka, A., Malato, S., Parsons, S.A., Poullos, I. & Mantzavinos, D., Advanced oxidation processes for water treatment: advances and trends for R&D. *Journal of Chemical Technology and Biotechnology*, **83**, pp.769-776, 2008.
- [9] Oppenlander, T., Photochemical purification of water and air. Advanced Oxidation Processes (AOPs): Principles, reaction mechanisms. *Reactor Concepts*, 2003.
- [10] Petrovic, M., Radjenovic, J. & Barcelo D., Advanced oxidation processes (AOPs) applied for wastewater and drinking water treatment. Elimination of pharmaceuticals. *The Holistic Approach to Environment*, **1**(2), pp. 63-74, 2011.
- [11] Zhou, H. & Smith D.W., Advanced technologies in water and wastewater treatment. *Journal of Environmental Engineering and Science*, **1**, pp. 247-264, 2002.
- [12] Stasinakis, A.S., Use of selected advanced oxidation processes (AOPs) for wastewater treatment – a mini review. *Global NEST Journal*, **10**(3), pp. 376-385, 2008.
- [13] Gogate, P.R. & Pandit, A.B., A review of imperative technologies for wastewater treatment II: hybrid methods. *Advances in Environmental Research*, **8**(3), pp. 553-597, 2004.
- [14] Hou, Y., Qu, J., Zhao, X., Lei, P., Wan, D. & Huang C.P., Electro-photocatalytic degradation of acid orange II using a novel TiO<sub>2</sub>/ACF photoanodes. *Science of the Total Environment*, **407**, pp. 2431-2439, 2009.
- [15] Neelavannan, M.G. & Ahmed Basha C., Electrochemical-assisted photocatalytic degradation of textile wastewater. *Separation and Purification Technology*, **61**, pp. 168-174, 2008.
- [16] Quan, X., Ruan, X., Zhao, H., Chen, S. & Zhao, Y., Photoelectrocatalytic degradation of pentachlorophenol in aqueous solution using TiO<sub>2</sub> nanotube film electrode. *Environmental Pollution*, **147**(2), pp. 409-414, 2007.
- [17] Chen, M.L., Zhang, F.J. & Oh, W.C., Synthesis, characterization, and photocatalytic analysis of CNT/TiO<sub>2</sub> composites derived from MWCNTs and titanium sources. *New Carbon Materials*, **24**(2), pp. 159-166, 2009.
- [18] Zhang, F.J., Chen, M.L., Lim, C.S. & Oh, W.C., Fabrication of CNT/TiO<sub>2</sub> electrodes and their photoelectrocatalytic properties for methylene blue degradation. *Journal of Ceramic Processing Research*, **10**(5), pp. 600-605, 2009.
- [19] Manea, F. et al., Voltammetric detection of urea on an Ag-modified zeolite-expanded graphite-epoxy composite electrode. *Sensors*, **8**, pp. 5806-5819, 2008.
- [20] Carvalho, R.H., Lemos, M.A.N.D.A., Lemos, F., Cabral, J.M.S. & Riberio, F.R., Electro-oxidation of phenol on zeolite/graphite composite electrodes Part 3. Influence of the electrolyte and of nonelectroactive cations. *Catalysis Today*, **133-135**, pp. 855-862, 2008.



- [21] Vlaicu, I., Pop, A., Manea, F. & Radovan, C., Degradation of humic acid from water by advanced electrochemical oxidation method. *Water Science and Technology: Water Supply*, **11**(1), pp. 85-95, 2011.
- [22] Baciuc, A., Remes, A., Ilinoiu, E., Manea, F., Picken, S.J. & Schoonman, J., Carbon nanotubes composite for environmental friendly sensing. *Environmental Engineering and Management Journal*, **11**(2), pp. 1967-1974, 2012.

